JOURNAL OF
Materials
CHEMISTRY

Unusual adsorption mechanism for carboxylic acid gases by polyamine-intercalated α-zirconium phosphate

Hirokazu Nakayama,*[a] Aki Hayashi,[a] Taro Eguchi,[b] Nobuo Nakamura[b] and Mitsutomo Tsuhako[a]

[a]*Department of Functional Molecular Chemistry, Kobe Pharmaceutical University, Kobe 658-8558, Japan. E-mail: hiro@kobepharma-u.ac.jp*
[b]*Department of Chemistry, Graduate School of Science, Osaka University, Toyonaka 560-0043, Japan*

Received 4th February 2002, Accepted 18th July 2002
First published as an Advance Article on the web 28th August 2002

The adsorption mechanism of gaseous carboxylic acid by diethylenetriamine- or pentaethylenehexamine-intercalated α-zirconium phosphate was examined in detail using XRD and solid-state ^{13}C and ^{31}P NMR. The adsorption of acetic acid, propanoic acid, and butyric acid resulted in the co-intercalation of the carboxylic acid molecules into polyamine-intercalated α-zirconium phosphate to expand their interlayer distance by 0.64–0.97 nm. In the case of formic acid, its adsorption induced the rearrangement of the polyamine molecules within the interlayer space.

Following the initial synthesis of layered zirconium phosphates by Clearfield *et al.* in the 1960's,[1,2] extensive studies were carried out in the 1970's to investigate the ion-exchange capability of these compounds. Recently, inorganic–organic hybrid materials based on layered phosphates and clays have been synthesized in efforts to produce materials with novel functionalities.[3] As examples, silica-pillared zirconium phosphate for a highly dispersed metal oxide catalyst[4] and *p*-nitroaniline intercalated kaolinite with high SHG intensity[5] have been recently reported.

Pollution of the environment by harmful substances is a serious problem, and it has been the objective of many researchers to synthesize new types of materials that can effectively adsorb harmful substances. To this end, functionalized porous silica as heavy metal adsorbents,[6] pyrene sorption by organic compounds intercalated layered double-metal hydroxide,[7] and adsorption of alcohol by silylated magadiite[8] have been investigated. Recently, we reported that polyamine-intercalated layered phosphates can adsorb considerable amounts of gaseous aldehydes and carboxylic acids; however the adsorption mechanism was not described in detail.[9] Although it is remarkable for modified α-zirconium phosphate, which is known as a solid acid, to adsorb considerable amounts of gaseous carboxylic acids, our studies have shown that this can be achieved by simple modification of layered phosphate by the intercalation of polyamine and that the amount of adsorption can be controlled by the degree of modification. Herein we report on the adsorption mechanism of gaseous carboxylic acid by diethylenetriamine- and pentaethylenehexamine-intercalated α-zirconium phosphates using X-ray powder diffraction (XRD) and solid-state ^{31}P and ^{13}C NMR. To the best of our knowledge, this is the first such report describing the adsorption of gaseous acid by modified zirconium phosphate accompanied by the intercalation of acid molecules.

Experimental

Reagent-grade diethylenetriamine (abbreviated as 2E3A), pentaethylenehexamine (5E6A), formic acid, acetic acid, propanoic acid, and *n*-butyric acid were purchased from Wako Chemicals Co., Ltd. [^{13}C]Formic acid (99%) was purchased from Cambridge Isotope Laboratories, Inc. α-Zirconium phosphate monohydrate (α-Zr(HPO$_4$)$_2$·H$_2$O; abbreviated as α-ZrP) was prepared according to reported procedures.[10] 2E3A-intercalated α-ZrP was prepared according to procedures described in a previous report.[11] 5E6A-intercalated α-ZrP was prepared by mixing α-ZrP (1 g) in a 0.01 M 5E6A aqueous solution (100 mL) with agitation at 80 °C for 1 week.

Adsorption experiments using 2E3A- or 5E6A-intercalation compounds (0.3 g) were carried out in the saturated vapor of the carboxylic acids in a closed glass device (Fig. 1), which was placed in an incubator and maintained at the prescribed temperature (±0.1 °C). The amount of adsorption was calculated by determining the overall increase in the weight of the intercalation compound. Following the maximum adsorption of the carboxylic acid, the carboxylic acid adhered to the surface was removed from the sample using a vacuum (homemade vacuum line; 10^{-3} bar) in preparation for XRD and solid-state NMR measurements. This avoids the observation of surface adsorbed species by instrumental measurements.

Powder X-ray diffraction (XRD) patterns were measured using a Rigaku Denki Rint 2000 diffractometer *via* Ni-filtered Cu-Kα radiation. The amounts of 2E3A and 5E6A intercalated into α-ZrP were determined by elemental analyses using a Sumigraph NC-90A. Solid-state ^{31}P MAS and ^{13}C CP/MAS NMR spectra of the intercalation compounds were obtained using a Bruker DSX-200 spectrometer operating at 81.0 MHz for ^{31}P NMR and 50.2 MHz for ^{13}C NMR. A single pulse

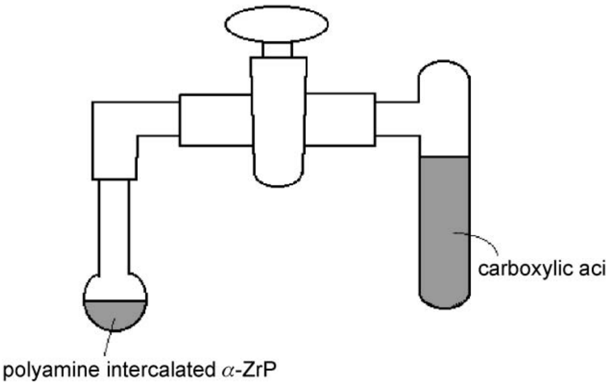

Fig. 1 Home-made glass device for adsorption experiment.

sequence with a $\pi/2$ pulse of 2 μs with ^{1}H high-power decoupling was used for ^{31}P magic angle spinning (MAS) NMR spectra. For ^{31}P MAS NMR spectra, 8 FIDs with a recycle time of 20 s were sufficient to obtain spectra with reasonable signal to noise (S/N) ratios. A cross-polarization (CP) pulse sequence with ^{1}H high-power decoupling was used to obtain ^{13}C CP/MAS NMR spectra. ^{13}C CP/MAS NMR spectra were acquired by accumulating 900 FIDs with a recycle time of 4 s. The MAS rate was 3–4 kHz. An 85% H_3PO_4 aqueous solution and TMS were used as reference for ^{31}P and ^{13}C NMR, respectively.

Results and discussion

Adsorption of carboxylic acids

As reported in a previous paper, various types of polyamine-intercalated layered phosphates were shown to adsorb acetic acid gas.[9] However, it is remarkable for modified α-zirconium phosphate, which is known as a solid acid, to adsorb gaseous carboxylic acids. In order to investigate this curious adsorption mechanism microscopically, preparation of the intercalation compounds with a uniform phase was preferable. As shown in a previous paper,[11] by controlling the reaction time, two different phases of 2E3A-intercalated α-ZrP were isolated as single compounds (Phase I and Phase II), each of which behaved differently in the adsorption of carboxylic acids.[11] In addition, the intercalation compound using 5E6A, which has a longer alkyl chain and more amino groups than 2E3A, was prepared to investigate the effect of polyamine on the properties of the intercalated compounds and the adsorption mechanism. Following procedures described earlier, a single phase 5E6A-intercalated α-ZrP was obtained at 80 °C.

Fig. 2 illustrates the schematic structural models of 2E3A-intercalated α-ZrP (Phase I and Phase II) and 5E6A-intercalated α-ZrP, as estimated from XRD, and ^{31}P and ^{13}C solid-state NMR.[11] Although Phase I and Phase II are both 2E3A-intercalated α-ZrP, the arrangement and the uptake of 2E3A in the interlayer space of α-ZrP were different for the two phases. For Phase II (Fig. 2(b)), the uptake of 2E3A was 0.82 mole per mole of α-ZrP, which indicates that the majority of the protons of the HPO_4 groups of α-ZrP reacted with the terminal amino groups of 2E3A *via* an acid–base reaction, and that the 2E3A molecule exists as the all-*trans* conformation within the interlayer space (d = 1.57 nm).[11] On the other hand, the uptake of 2E3A for Phase I (Fig. 2(a)) was 0.46 mole per mole of α-ZrP, which suggests that half of the protons of the HPO_4 groups have no interactions with the amino groups of 2E3A, and that the 2E3A molecule exists as a bent structure within the interlayer space (d = 1.02 nm).[11] For 5E6A-intercalated α-ZrP (Fig. 2(c)), the uptake of 5E6A was 0.34 mol, which is comparable to that of Phase I. The 5E6A molecule exists as a bent structure, almost at the center of the interlayer space (d = 1.68 nm).

The time dependence of the adsorption amounts of carboxylic acids for 2E3A- or 5E6A-intercalated α-ZrP are shown in Fig. 3. The adsorptions using formic acid, acetic acid, and propanoic acid were carried out at 40 °C, and butyric acid at 60 °C. Vapor pressures of the organic acids at the stated temperatures were 98, 40, 10, and 10 mmHg, respectively. As shown in Fig. 3, the adsorption behavior of formic acid differed significantly from those of the other carboxylic acids. For Phase I, except for formic acid, the adsorption amounts of the carboxylic acids were less than 10%. On the other hand, Phase II and 5E6A-intercalated α-ZrP adsorbed gaseous carboxylic

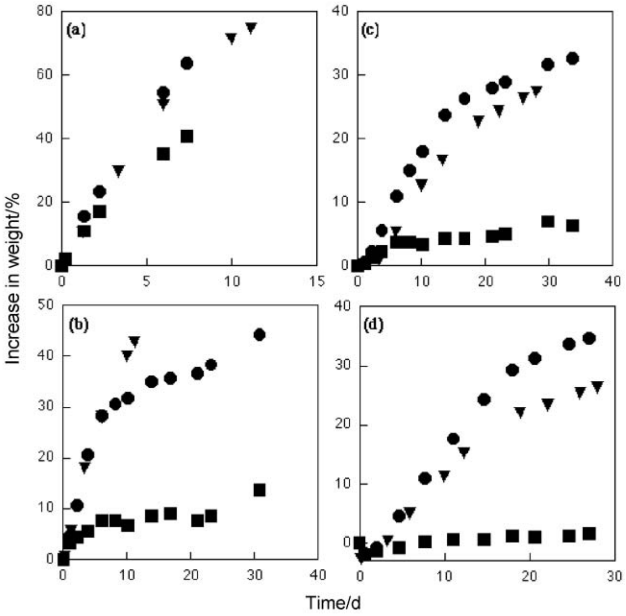

Fig. 3 Time dependence of the adsorption amounts of (a) formic acid, (b) acetic acid, (c) propanoic acid, and (d) butyric acid; Phase I (■), Phase II (●), and 5E6A-intercalated α-ZrP (▼).

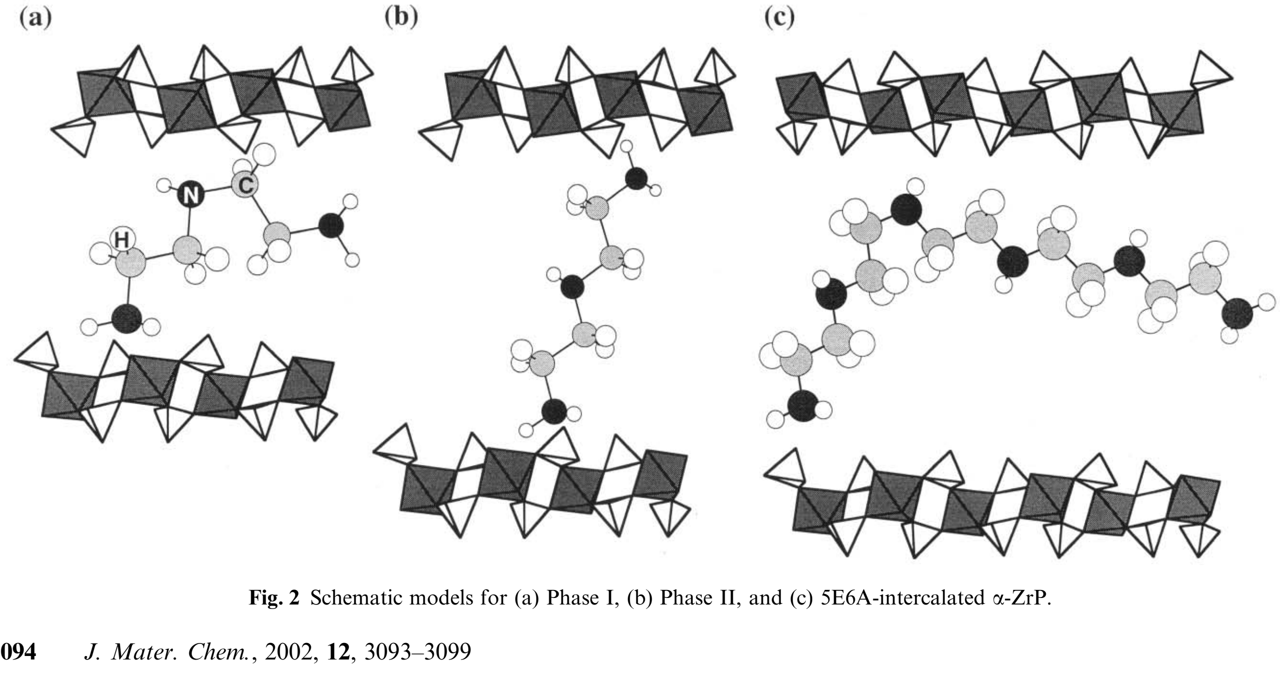

Fig. 2 Schematic models for (a) Phase I, (b) Phase II, and (c) 5E6A-intercalated α-ZrP.

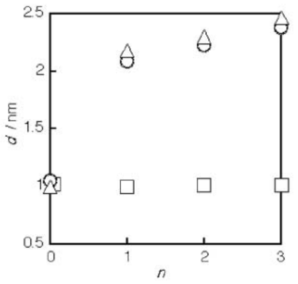

Fig. 4 Interlayer distances of Phase I (□), Phase II (○), and 5E6A-intercalated α-ZrP (△) following the adsorption of carboxylic acids; HCOOH (n = 0) or $CH_3(CH_2)_{n-1}COOH$ (n = 1–3). Actual interlayer spacing is $d - 0.76$ nm.

acids with increases of more than 30% in the overall weight of the intercalation compounds, implying the adsorption of one carboxylic acid molecule per polyamine molecule. For formic acid, Phase I adsorbed a comparable amount as that for Phase II and 5E6A-intercalated α-ZrP, which suggests that the adsorption mechanism of formic acid is different to that of other carboxylic acids

Adsorption mechanism for acetic acid, propanoic acid, and butyric acid

Fig. 4 shows the interlayer distances (*d*) of the intercalation compounds following the adsorption of carboxylic acids, as a function of the number of carbon atoms (*n*) in the alkyl chain of the acids. For Phase I, the interlayer distance (*d*) remained constant, in agreement with the lack of adsorption which was shown in Fig. 3. In contrast, following the adsorption of gaseous carboxylic acid, the interlayer distances (*d*) of Phase II and 5E6A-intercalated α-ZrP increased linearly with increasing alkyl chain length (*n*), and can be expressed using the following equations for Phase II [eqn. (1)] and 5E6A-intercalated α-ZrP [eqn. (2)], respectively, where n = 1–3:

$$d = 1.92 + 0.15n \tag{1}$$

$$d = 2.05 + 0.15n \tag{2}$$

The systematic expansion of the interlayer distances implied that the adsorption of the carboxylic acid molecules resulted in their co-intercalation within the interlayer spaces of Phase II or 5E6A-intercalated α-ZrP. Furthermore, the carboxylic acid molecules were arranged identically for all of the carboxylic acids and the two phases.

As previously reported,[12–15] solid-state NMR can give an insight into the nature of the interactions within the interlayer space of the layered phosphate. In order to identify the co-intercalation mechanisms of Phase I, Phase II, and 5E6A-intercalated α-ZrP microscopically, ^{31}P and ^{13}C solid-state NMR studies were undertaken, and the resulting ^{31}P MAS NMR spectra following the adsorption of the carboxylic acids are shown in Fig. 5. In the case of Phase I, the NMR spectra remained unchanged following the adsorption of carboxylic acid gases; this is reasonable and consistent with the results of uptake and XRD, which show that Phase I adsorbed only a small amount of carboxylic acid. On the other hand, drastic changes in the NMR spectra were observed for Phase II and 5E6A-intercalated α-ZrP. For Phase II, before the introduction of the carboxylic acids, the two terminal amino groups of the 2E3A molecule (all-*trans* conformation and deprotonated phosphate group), formed a $NH_3^+\cdots{}^-O$–P bond[11] at both ends of the 2E3A molecule (Fig. 2(b)), which induced a downfield shift to −15.7 ppm of the single peak (−18.7 ppm for α-ZrP).[16] Upon adsorption of the carboxylic acids, this downfield shift was not observed, and the signal reappeared at −18 ppm, which was attributed to the reprotonation of the phosphate group by the co-intercalated carboxylic acid molecule.[12–15,17] For 5E6A-intercalated α-ZrP, two ^{31}P signals were observed; the signal at −15.5 ppm was assigned to the ionized phosphate group due to the protonation of the terminal amino group in the formation of a $NH_3^+\cdots{}^-O$–P bond, similar to Phase II (Fig. 2(b)),[6] whereas the signal at −18.0 ppm was assigned to the free (or non-deprotonated) phosphate group which interacts weakly with the amino group. However, following the adsorption of the carboxylic acids, the low field signal at −15.5 ppm disappeared completely, whereas the signal at −18 ppm remained, implying an upfield shift of the signal from −15.5 ppm to −18 ppm,[17] which again can be explained by the reprotonation of the PO_4 groups by the co-intercalated carboxylic acid. Therefore, the adsorption of gaseous carboxylic acids by Phase II and 5E6A-intercalated α-ZrP resulted in the insertion of the carboxylic acid molecules

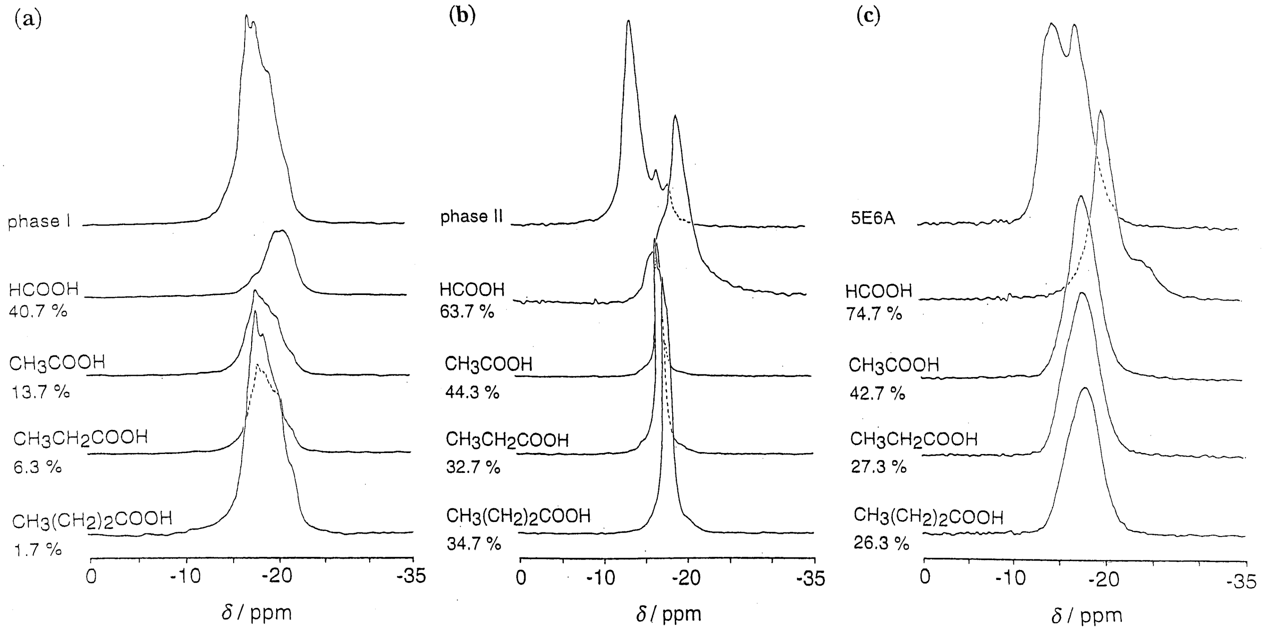

Fig. 5 ^{31}P MAS NMR spectra of (a) Phase I, (b) Phase II, and (c) 5E6A-intercalated α-ZrP before and after adsorption of the carboxylic acids. The values listed below the names of adsorbed gases are the increases in weight.

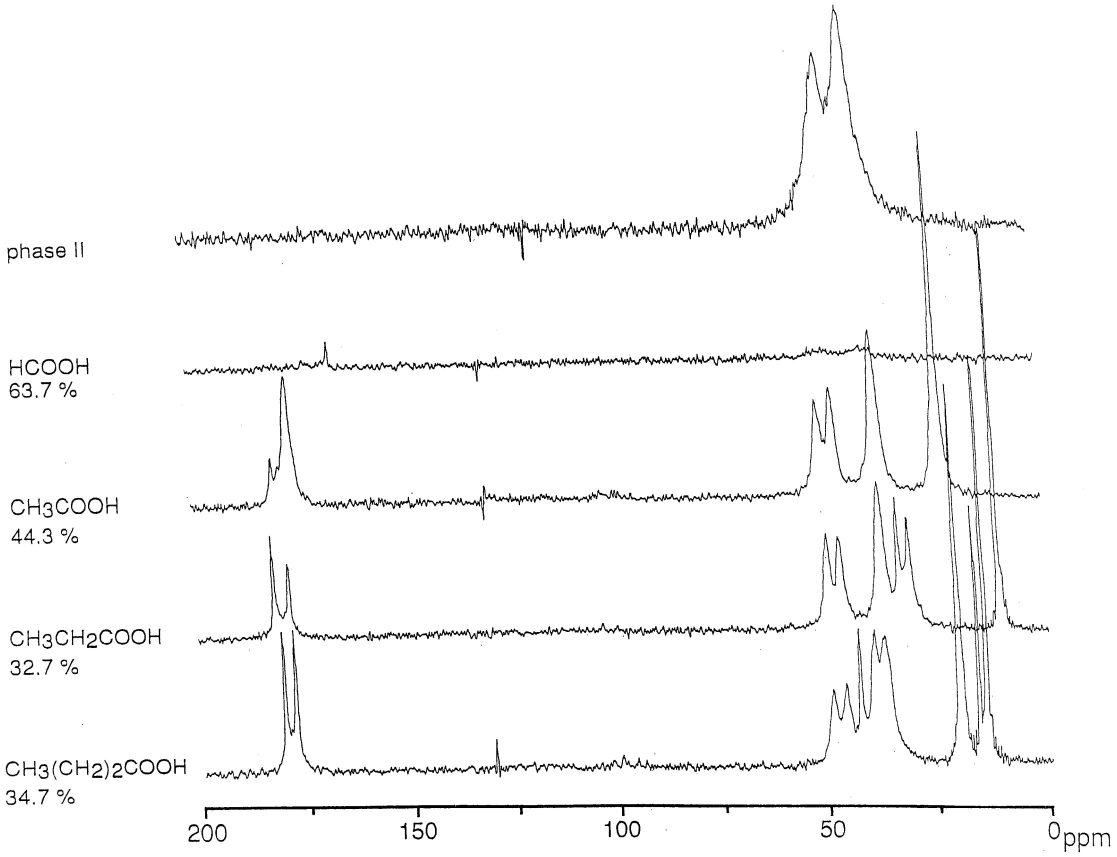

Fig. 6 ^{13}C CP/MAS NMR spectra of Phase II before and after adsorption of the carboxylic acids. The values listed below the names of adsorbed gases are the increases in weight.

between the terminal amino groups and the layered phosphates, with the reprotonation of the PO_4 group.

These results are supported by subsequent ^{13}C CP/MAS NMR studies, as shown in Figs. 6 and 7. For Phase II, only two signals were expected because the two α and β carbons of the 2E3A molecule are equivalent within the interlayer space of Phase II due to its symmetric conformation, as shown in Fig. 2(b), and accordingly two signals (45 and 39 ppm) were observed. Following the adsorption of the carboxylic acid, the α and/or β carbon signals of the 2E3A molecule were observed as doublets, probably due to the loss of the symmetric configuration of the 2E3A molecule resulting from the insertion of a carboxylic acid molecule at one end of the 2E3A molecule. Although this model seems to contradict the observation of a single ^{31}P signal following the adsorption of carboxylic acid, insertion of a carboxylic acid may induce a shift of the 2E3A molecule, causing the amino group to interact with two phosphate groups, as shown in Fig. 8(a). This might be the origin of the equivalence of the two phosphate groups. Furthermore, as shown in Fig. 6, carboxylic acid signals were observed. In addition to the signals of α carbon (49, 46 ppm) and the signal of β carbon (36 ppm), signals at 22.1 ppm ($-CH_3$) and 177.5 ppm ($-COOH$) for acetic acid, and those at 10.5 ($-CH_3$), 29.7, 32.1($-CH_2-$), and 178.9, 182.4 ppm ($-COOH$) for propanoic acid were observed. For butyric acid, the signal splittings of the α carbon (48, 45 ppm) and β carbon (38, 36 ppm) of the 2E3A molecule were observed together with signals at 14.0, 15.8 ($-CH_3$), 19.8, 42.0 ($-CH_2-$), and 178.6, 181.2 ppm ($-COOH$) of butyric acid. For propanoic acid and butyric acid, the splittings of some signals were attributable to crystal effects, which sometimes appear due to inequivalency of the molecules (solid effect), although the reason for why there is no splitting of the signals of acetic acid is uncertain. As shown in Fig. 7, a broad signal between 38 and 55 ppm was observed for 5E6A-intercalated α-ZrP, which corresponds to the non-symmetric conformation of the 5E6A molecule, as shown in Fig. 2(c). Following adsorption, carboxylic acid signals were observed at around 10–20 ppm and at 180 ppm, which were similar to those of Phase II. The signal intensities due to the carboxylic acids were comparable to those due to 2E3A and 5E6A carbons, which suggests that the number of adsorbed carboxylic acid molecules is comparable to the numbers of 2E3A or 5E6A molecules. Similar signal intensities of the carboxylic acids to those of the polyamines, and the splitting of some signals due to crystal effects suggest that the adsorption of carboxylic acids is not simply surface adsorption, but rather insertion of the carboxylic acid molecules, and that the carboxylic acid molecules are rigidly arranged within the interlayer space. This explanation is consistent with the uptake measurements, which indicated the adsorption of one carboxylic acid molecule per polyamine molecule by XRD, and the shifts in the ^{31}P NMR signal following the adsorption of the carboxylic acids.

Solid state NMR and XRD data strongly indicate that the adsorption of gaseous carboxylic acids, except for formic acid, by Phase II and 5E6A-intercalated α-ZrP resulted in the insertion of the carboxylic acid molecules between the terminal amino groups and the phosphate layers. Schematic models for the adsorptions are shown in Fig. 8.

Adsorption mechanism of formic acid

In contrast to the other carboxylic acids, formic acid, which could proceed through a different adsorption mechanism, underwent adsorption on Phase I, in amounts that are comparable to those on Phase II and 5E6A-intercalated α-ZrP, as shown in Fig. 3. Although considerable amounts of formic acid were adsorbed, the interlayer distance remained unchanged at

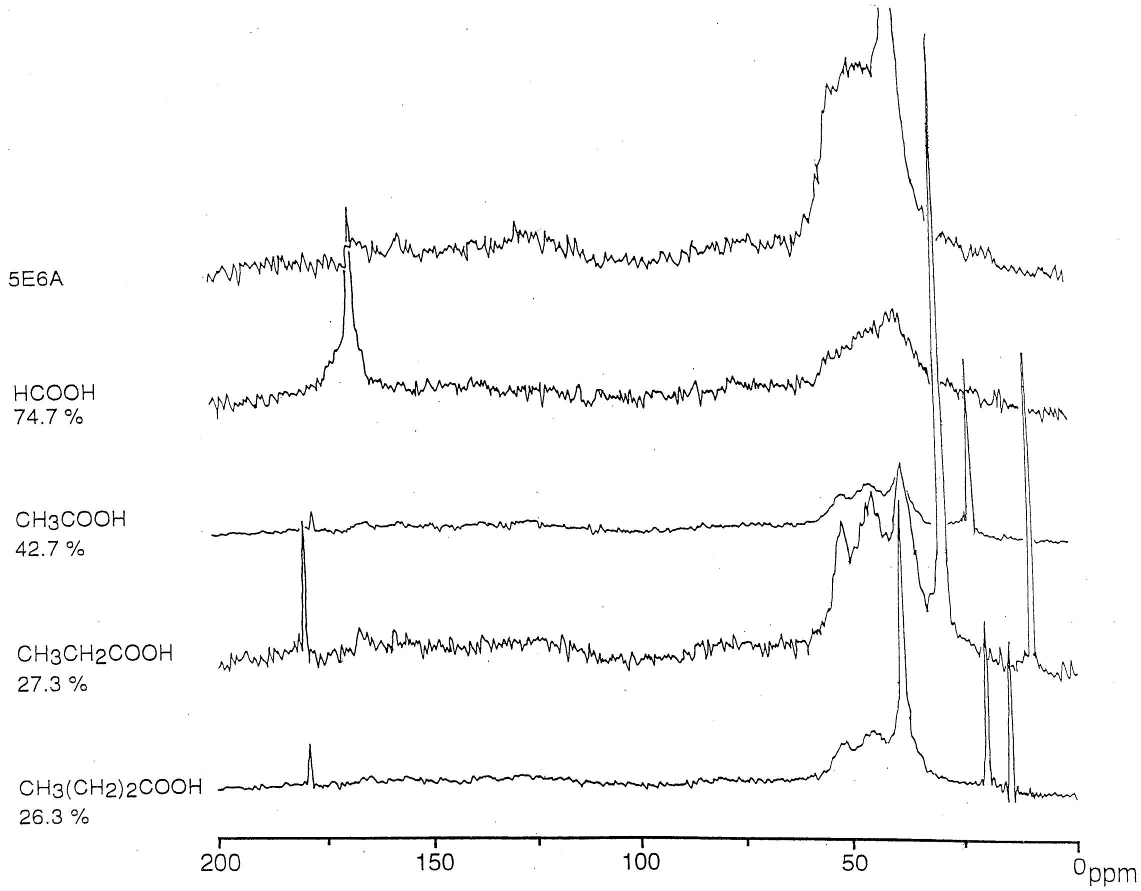

Fig. 7 ^{13}C CP/MAS NMR spectra of 5E6A-intercalated α-ZrP before and after adsorption of the carboxylic acids. The values listed below the names of adsorbed gases are the increases in weight.

1.0 nm for Phase I (Fig. 4). For Phase II and 5E6A-intercalated α-ZrP, interlayer distances of 1.0 nm were observed, suggesting that the adsorption mechanism of formic acid by 2E3A- or 5E6A-intercalated α-ZrP differs considerably from those of the other carboxylic acids. The interlayer distances for Phase I, Phase II, and 5E6A-intercalated α-ZrP of 1.0 nm following the

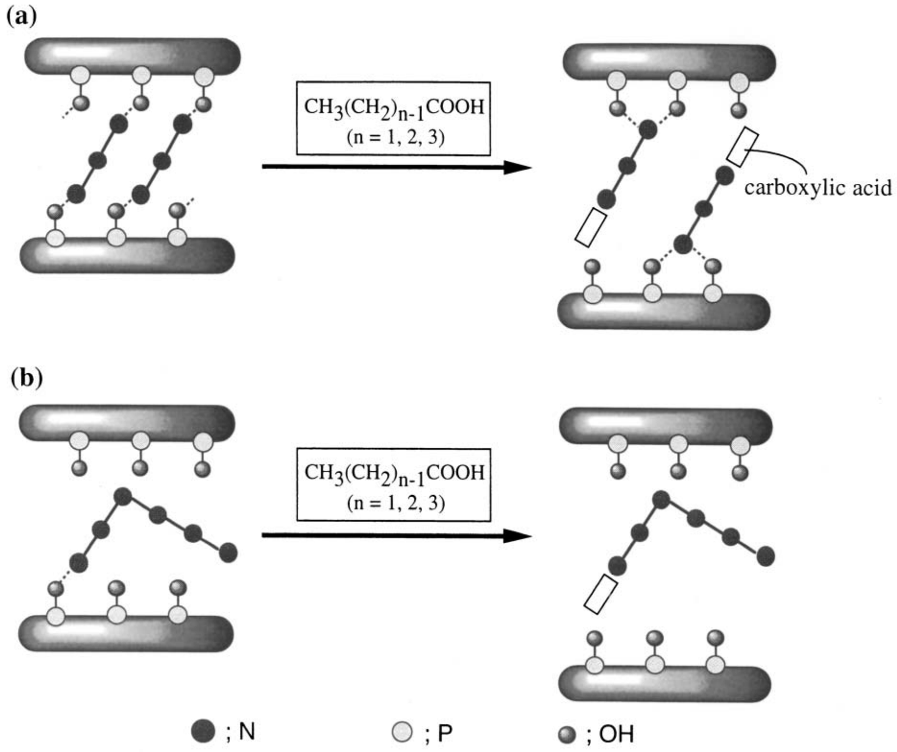

Fig. 8 Schematic models of carboxylic acid adsorption in (a) Phase II and (b) 5E6A-intercalated α-ZrP.

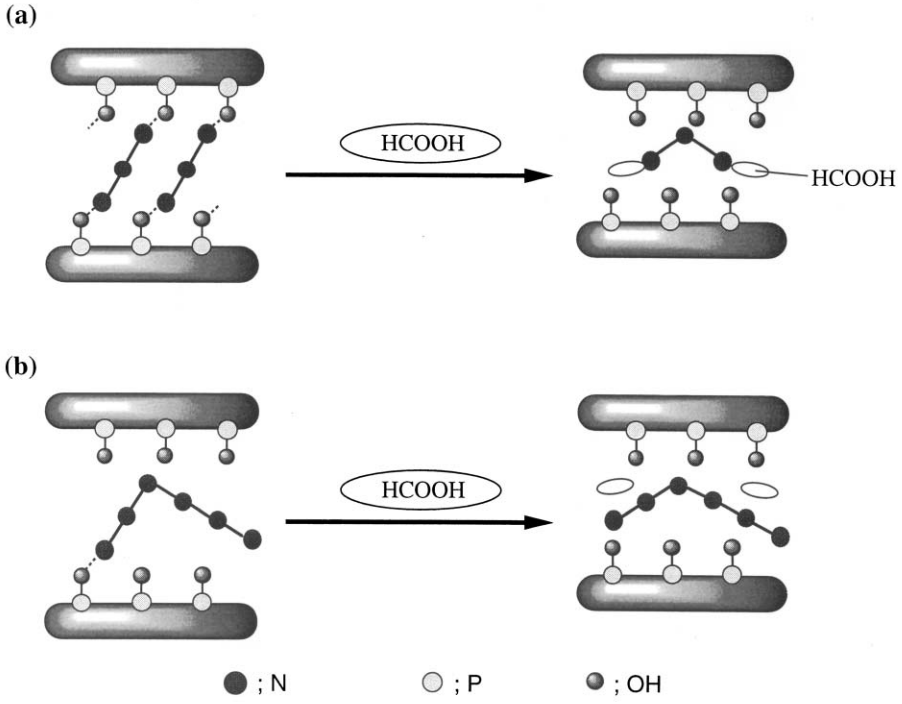

Fig. 9 Schematic models of formic acid adsorption in (a) Phase II and (b) 5E6A-intercalated α-ZrP.

adsorption of formic acid suggests that the conformations of 2E3A in Phase II and 5E6A were changed by the adsorption of formic acid, as shown in Fig. 9.

Similar effects were demonstrated by ^{31}P MAS NMR studies. As shown in Fig. 5, for Phase II and similarly for 5E6A-intercalated α-ZrP following adsorption of formic acid, the native signals (−15.7 ppm) disappeared completely, and in their place a broad signal (−21 ppm) was observed. Comparable upfield shifts from the original α-ZrP (−18.7 ppm) have been reported for *n*-alkylamine intercalation compounds of α-ZrP with low-loading of the amine.[17] Under low-loading conditions, the *n*-alkylamine molecule is intercalated in an arrangement that is almost parallel to the phosphate layer. In contrast, under high-loading conditions, interactions between the amino and phosphate groups are stronger, and accordingly the ^{31}P NMR signal shows a downfield shift (−15.7 ppm). The upfield shift observed following the adsorption of formic acid supports the conformational changes as shown in Fig. 9.

Although we have observed the changes in the conformations of 2E3A in Phase II and of 5E6A in the intercalated α-ZrP following the adsorption of the formic acid, the actual adsorption sites of the formic acid molecules remain unclear. ^{13}C CP/MAS NMR spectra of compounds following formic acid adsorption exhibited a weak signal at 175 ppm (Figs. 6 and 7), although the adsorption amounts were 40.7, 63.7, and 74.7% for Phase I, Phase II, and 5E6A-intercalated α-ZrP, respectively. It is well known that formic acid can exhibit characteristics of formaldehyde, and in our case, adsorption may also be accompanied by a catalytic decomposition reaction.[18] Therefore to identify the formic acid adsorption as a physical adsorption or decomposition reaction, the adsorption experiment was carried out using ^{13}C-labeled formic acid. As shown in the ^{13}C CP/MAS NMR spectra in Fig. 10, although different splittings due to different adsorption sites for three intercalation compounds were evident, only the signal due to formic acid was observed; signals due to decomposed compounds were not detected. These results show that adsorption does not occur through a catalytic decomposition reaction but through physical adsorption, and that although the adsorption site is not yet defined, formic acid is co-intercalated within the free space, as shown in Fig. 9.

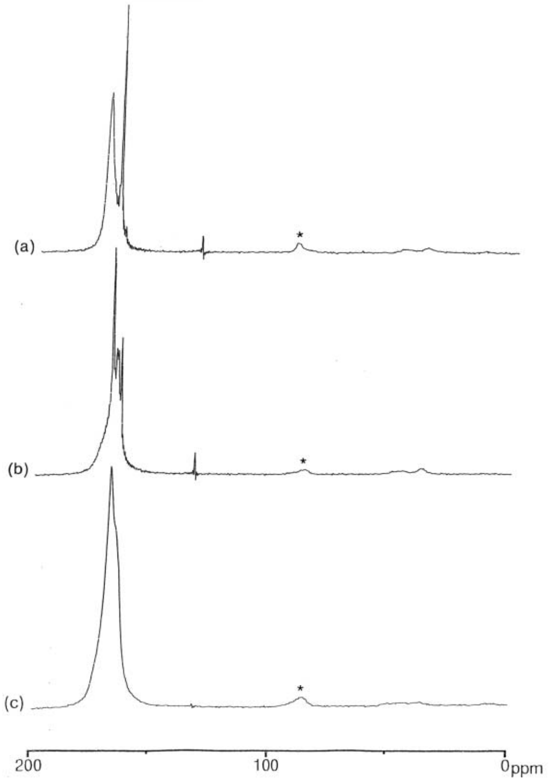

Fig. 10 ^{13}C CP/MAS NMR spectra of [^{13}C]formic acid adsorbed in (a) Phase I, (b) Phase II, and (c) 5E6A-intercalated α-ZrP. Amounts of adsorption are (a) 39.7, (b) 41, and (c) 38%, respectively. *spinning side band

Origin of adsorption

In the cases of acetic, propanoic, and butyric acids, adsorption results in the co-intercalation of the carboxylic acid molecules into Phase II and 5E6A-intercalated α-ZrP. This adsorption is remarkable for the following reason: although solid acid α-ZrP is a stronger acid than carboxylic acid, carboxylic acid molecules are adsorbed onto α-ZrP. Upon adsorption, the carboxylic acid disrupts the interaction between amino group and acidic phosphate. The interlayer space of layered phosphate and the acidity of the co-intercalation compound (carboxylic acid) may play significant roles in the adsorption mechanism. For Phase I, the interlayer distance (1.08 nm) is too small to co-intercalate the carboxylic acid molecules, and furthermore, only half of the protons of the phosphate groups in α-ZrP react with the 2E3A molecules. Therefore, the intercalation compound of Phase I showed acidic character, which hampered the co-intercalation of the carboxylic acids. On the other hand, for Phase II and 5E6A-intercalated α-ZrP, the interlayer distances (1.58 and 1.68 nm, respectively) were sufficiently large for the carboxylic acid molecules to penetrate. Also, Phase II and 5E6A-intercalated α-ZrP are not acidic, since the phosphate protons of α-ZrP were neutralized by the amino groups. Although the driving force for the adsorption of carboxylic acids is not clear, the low barrier to adsorption by neutralization of the acidic α-ZrP by the polyamine and expansion of the interlayer distance allowed the co-intercalation of the carboxylic acids.

In the case of formic acid, because Phase I was shown to adsorb formic acid at levels comparable to those of Phase II and 5E6A-intercalated α-ZrP, the interlayer distance may not be a key factor in the adsorption mechanism. In fact, the adsorption might be due to the small size of the formic acid molecule; following the adsorption of formic acid, all the intercalation compounds attain an interlayer distance of about 1.0 nm. In contrast to the regular expansion as seen for other carboxylic acids with Phase II and 5E6A-intercalated in α-ZrP, no differences in the interlayer distances were observed. Since formic acid is the strongest acid among the carboxylic acids studied, its strong acidity may play an important role in the adsorption of formic acid in Phase I. Furthermore, the strong acidity of formic acid causes the disruption of the pillar arrangement of 2E3A in Phase II and 5E6A in 5E6A-intercalated in α-ZrP.

In conclusion, the adsorption of carboxylic acids resulted in its co-intercalation between the layered phosphate and the polyamine molecule. The adsorption capacity is regulated by the arrangement of the polyamine molecule within the interlayer region. In the case of formic acid, no differences in the adsorption properties of the three different intercalation compounds were observed.

Acknowledgement

The authors thank the Ministry of Education, Science, Sports, and Culture (No. 10650831) for a Grant-in-Aid for Scientific Research.

References

1 A. Clearfield and J. A. Stynes, *J. Inorg. Nucl. Chem.*, 1964, **26**, 117.

2 A. Clearfield, R. H. Blessing and J. A. Stynes, *J. Inorg. Nucl. Chem.*, 1968, **30**, 2249.

3 A. Clearfield and M. Costantino, *Comprehensive Supramolecular Chemistry*, ed. G. Alberti and T. Bein, Pergamon, Oxford, 1996, vol. 7, p. 107.

4 W. Wang, Y. Tang, M. Kapplen, N. He, W. Hua and Z. Gao, *Microporous Mesoporous Mater.*, 2001, **42**, 219.

5 K. Kuroda, K. Hiraguri, Y. Komori, Y. Sugahara, H. Mouri and Y. Uesu, *Chem. Commun.*, 1999, 2253.

6 B. Lee, Y. Kim, H. Lee and J. Yi, *Microporous Mesoporous Mater.*, 2001, **42**, 77.

7 P. K. Dutta and D. S. Robins, *Langmuir*, 1994, **10**, 1851.

8 M. Ogawa, S. Okutomo and K. Kuroda, *J. Am. Chem. Soc.*, 1998, **120**, 9291.

9 M. Danjo, A. Hayashi, H. Nakayama, Y. Kimira, T. Shimizu, Y. Mizuguchi, Y. Yagita, M. Tsuhako, H. Nariai and I. Motooka, *Bull. Chem. Soc. Jpn.*, 1999, **72**, 2079.

10 M. Tsuhako, Y. Horii, H. Nariai and I. Motooka, *Nippon Kagaku Kaishi*, 1987, 1541.

11 A. Hayashi, H. Nakayama, M. Tsuhako, T. Eguchi and N. Nakamura, *Mol. Cryst. Liq. Cryst.*, 2000, **341**, 573.

12 M. Danjo, M. Tsuhako, H. Nakayama, T. Eguchi, N. Nakamura, S. Yamaguchi, H. Nariai and I. Motooka, *Bull. Chem. Soc. Jpn.*, 1997, **70**, 1053.

13 H. Nakayama, M. Danjo, M. Tsuhako, T. Eguchi and N. Nakamura, *Phosphorus Res. Bull.*, 1999, **9**, 55.

14 A. Hayashi, H. Nakayama, M. Tsuhako, T. Eguchi and N. Nakamura, *J. Inclusion. Phenom.*, 1999, **34**, 401.

15 H. Nakayama, T. Eguchi, N. Nakamura, S. Yamaguchi, M. Danjo and M. Tsuhako, *J. Mater. Chem.*, 1997, **7**, 1063.

16 N. J. Clayden, *J. Chem. Soc., Dalton Trans.*, 1987, 1877.

17 D. J. MacLachlan and K. R. Morgan, *J. Phys. Chem.*, 1990, **94**, 7656; D. J. MacLachlan and K. R. Morgan, *J. Phys. Chem.*, 1992, **96**, 3458.

18 H. Nakayama, A. Hayashi, T. Eguchi, N. Nakamura and M. Tsuhako, *Solid State Sci.*, 2002, **4**, 1067.